BIOCHEMISTRY
including biophysical chemistry & molecular biology

Article

pubs.acs.org/biochemistry

Structure and Dynamics of the Fish Eye Lens Protein, γM7-Crystallin

Bryon Mahler,[†,§] Yingwei Chen,[‡,§] Jason Ford,[†] Caleb Thiel,[†] Graeme Wistow,*[,‡] and Zhengrong Wu*[,†]

[†]Department of Chemistry and Biochemistry, The Ohio State University, Columbus, Ohio 43210, United States

[‡]Section on Molecular Structure and Function, National Eye Institute, National Institutes of Health, Bethesda, Maryland 20892, United States

ABSTRACT: The vertebrate eye lens contains high concentrations of crystallins. The dense lenses of fish are particularly abundant in a class called γM-crystallin whose members are characterized by an unusually high methionine content and partial loss of the four tryptophan residues conserved in all γ-crystallins from mammals which are proposed to contribute to protection from UV-damage. Here, we present the structure and dynamics of γM7-crystallin from zebrafish (*Danio rerio*). The solution structure shares the typical two-domain, four-Greek-key motif arrangement of other γ-crystallins, with the major difference noted in the final loop of the N-terminal domain, spanning residues 65−72. This is likely due to the absence of the conserved tryptophans. Many of the methionine residues are exposed on the surface but are mostly well-ordered and frequently have contacts with aromatic side chains. This may contribute to the specialized surface properties of these proteins that exist under high molecular crowding in the fish lens. NMR relaxation data show increased backbone conformational motions in the loop regions of γM7 compared to those of mouse γS-crystallin and show that fast internal motion of the interdomain linker in γ-crystallins correlates with linker length. Unfolding studies monitored by tryptophan fluorescence confirm results from mutant mouse γS-crystallin and show that unfolding of a βγ-crystallin domain likely starts from unfolding of the variable loop containing the more fluorescently quenched tryptophan residue, resulting in a native-like unfolding intermediate.

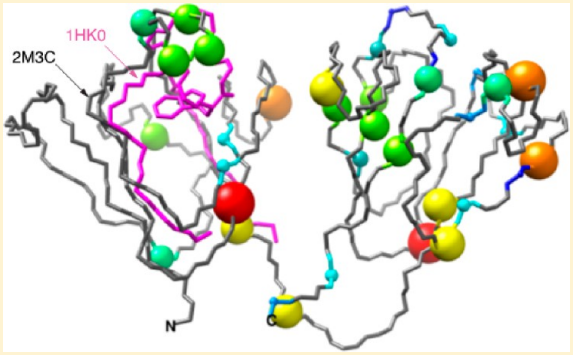

The related β- and γ-crystallins (belonging to a βγ-crystallin superfamily) are major protein components of the fiber cells in vertebrate lenses, where they contribute to the high concentration and short-range order responsible for providing both transparency and high refractive index to the lens.[1] These proteins share a common structure of a pair of domains each consisting of two intercalating Greek Key (GK) motifs. The proteins typically have high thermodynamic stability[2] and a delicate balance of surface properties for optimal solubility.[3]

Fish are the oldest and most diverse group of vertebrates. Because of the lack of corneal refractive power in water, fish lenses have a significantly higher refractive index compared to that of land vertebrates. The dominant fish lens proteins, γM-crystallins, are thought to be particularly adapted for dense packing in these hard lenses.[4,5] Alignment of α, β, and γ with other known Crystallin sequences indicates that fish γM-crystallins form a distinct group that differs from those of mammals by lacking conserved tryptophan pairs in each domain and possessing a very high methionine content.[6,7] The tryptophan pairs have been proposed to protect the retina from UV damage by absorbing and quenching longer wavelength ultraviolet,[8,9] an advantage for land vertebrates but perhaps less important for aquatic species. Even in mammalian γ-crystallins, the content of sulfur-containing residues is high, but this is greatly exceeded in fish γM-crystallins. It has been speculated that high methionine content might contribute to protein stability[10] and in mediating intermolecular interactions that may enhance solubility and dense protein packing in lenses.[7,11] Recent studies have also suggested that the high abundance of methionine is consistent with the requirement for the high refractive index of crystallins in lens.[12,13] Proteins with a high content of amino acids with high refractive index increments can achieve higher overall refractive power at relatively lower protein concentration and reduced osmotic pressure.[14] Indeed, other proteins with exceptionally high refractive index such as the S-crystallins from cephalopods[15,16] and reflectins from squid[17,18] are also highly enriched with methionine and contain a limited content of residues with low refractive index increment.[12]

Lens crystallins, upon mutation, post-translational modification, and/or an encounter with a denaturing environment, may go through a distinct unfolding pathway by forming partially unfolded intermediate(s),[19] similar to many serious protein deposition diseases,[20] resulting in opacity. For example, human γD- and γB-mutants can form a partially unfolded intermediate with one domain unfolded and the other intact,[21,22] while mutant mouse γS can conformationally exchange with a native-like intermediate under more physiologically relevant conditions.[23] Importantly, the partially unfolded crystallins have

Received: February 6, 2013
Revised: April 17, 2013
Published: April 18, 2013

been shown to trigger the formation of aggregates and/or fibrils *in vitro*.[24]

In these contexts, we have investigated the structure and the unfolding processes of the first γM-crystallin to be examined. While the solution structure of zebrafish γM7 topologically resembles that of other γ-crystallins from land vertebrates, significant local structural difference in the variable loop indicates that the conserved tryptophan residues are critical for the characteristic folding of the βγ-crystallin domain. By monitoring the distinct quenching properties of each tryptophan residue, we were able to show that the variable loops of the GK motif are more susceptible to unfolding, possibly representing a common unfolding pathway for all βγ-crystallin domains.

MATERIALS AND METHODS

Sample Preparation. The DNA encoding γM7 (pI 7.10) and γM2b (pI 8.02) was subcloned into the pET16b vector (Novagen) between NdeI and *Hin*dIII sites and transformed into *Escherichia coli* strain BL21(DE3)pLysS. Protein overexpression and purification has been carried out according to a previously detailed procedure.[25,26] Briefly, cells were grown at 37 °C until an absorbance at 600 nm of 0.6 and induced by 1 mM IPTG overnight. Cells were lysed by French press, and proteins were first purified by a fast flow Q anion exchange chromatography (GE Healthcare) in 25 mM Tris buffer (pH 8.5), 1 mM EDTA, and 1 mM DTT. Different from γS-crystallin, both γM7 and γM2b were eluted during extensive wash after flow through. These protein fractions were dialyzed overnight against 25 mM phosphate buffer (pH 6.2), 1 mM EDTA, and 1 mM DTT and further purified by monoS cation exchange chromatography (GE Healthcare). $^{15}NH_4Cl$ and/or ^{13}C-glucose was used as the sole nitrogen and carbon source for isotopically labeled γM7 for structure determination by NMR. Mutation of γM7 was achieved by site-directed mutagenesis using a QuickChange mutagenesis kit (Stratagene). The desired nucleotide sequence was confirmed by sequencing, and the resulting mutant was further verified by mass spectrometry.

Thermal Denaturation. Protein (0.5 mg/mL) in buffer was placed in a 1-mm path length cuvette, equilibrated for 1 min, and monitored by CD spectroscopy over a temperature range of 30−90 °C ramping at 2 °C/min. Each point was an average of three consecutive detections. The apparent fraction of unfolded protein (*Fu*) was calculated from the ellipticity as described by Pace,[27] using the expression: $Fu = (Y - Yn)/(Yu - Yn)$, where *Y* is the observed value, *Yu* and *Yn* are the values of the unfolded and native states, respectively. Peak signal at 218 nm from CD was used for data analysis.

Nuclear Magnetic Resonance Spectroscopy. Protein samples ranging from 0.8 to 2 mM in NMR buffer (25 mM imidazole-d_6, pH 6.2, 20 mM KCl, 2 mM DTT, 0.04% NaN_3, and 8% ^2H_2O) were obtained in a thin-wall Shigemi tube. All spectra were collected at 32 °C with Bruker Avance 600 and 800 MHz (^1H) NMR spectrometers equipped with *z*-axis gradient cryogenic probeheads. Backbone resonance assignments were made with standard heteronuclear triple resonance experiments,[28] and side chain assignments were determined by 3D HCCH-TOCSY and ^{15}N-TOCSY experiments.[29] The stereospecific assignments of the methyl side chains was determined from a sample grown in a media containing 10% ^{13}C-labeled glucose[30] and analyzed by the J-coupling modulated signals in a 2D $^1H-^{13}C$ constant-time HSQC experiment.[31] Interproton distance restraints were determined from 3D ^{15}N-edited NOESY-HSQC on a ^{15}N-labeled sample and 3D ^{13}C-edited HMQC-NOESY-HSQC (t_{mix} 120 ms) on a uniformly $^{15}N/^{13}C$-labeled sample in 100% ^2H_2O NMR buffer. Residual dipolar couplings $^1D_{NH}$ were measured with an interleaved HSQC and TROSY experiment using a uniformly ^{15}N-labeled sample partially aligned by a stretched 6% polyacrylamide gel.[32] Backbone ^{15}N T_1, T_2, and steady-state heteronuclear Overhauser effects (hnNOE) were collected at 600 MHz with a repetition delay of 2 s for all experiments. Relaxation delays in the T_1 experiments were 0.010, 0.085, 0.205, 0.330, 0.455, 0.605, 0.780, and 1.050 s, and CPMG mixing times in the T_2 measurements were 7.344, 14.688, 22.032, 29.376, 36.720, 44.064, 51.408, and 66.096 ms. NOE data were collected in an interleaved mode with and without a 3 s saturation period.[33] All data were processed with NMRPipe.[34] Resonance and NOE assignments were made with NMRViewJ.[35]

Structure Calculation. Backbone dihedral angle restraints were calculated from chemical shift assignments using the software package, TALOS+.[36] Distance restraint upper bounds were either 2.70, 3.50, or 5.00 Å as determined by the NOE cross-peak intensity and the lower bound was 1.80 Å. The structures were calculated from a simulated annealing protocol implemented in XPLOR-NIH.[37] Initial structures were calculated from random structures with decreasing dihedral angle (200 to 20 kcal/rad^2) and increasing NOE and hydrogen bonding (0.5 to 50 kcal/Å) force constants, and with van der Waals radii taken from 0.002 to 0.5 their calculated value, while the temperature was decreased from 1000 to 300 K in 5 K increments. The resulting structures were then subjected to further refinement with slow ramping down of the dihedral angle (100 to 10 kcal/rad^2), and gradual increasing of NOE and hydrogen bond (0.002 to 50 kcal/Å) and RDC (0.5 to 1.0 kcal/Hz^2) force constants and van der Waals radii (0.002 to 1.0 their calculated value), while the temperature was decreased from 1000 to 300 K in 5 K increments. The lowest energy structures were checked with PROCHECK-NMR.[38] All structure graphics were created with Chimera.[39]

Fluorescence Unfolding. Fluorescence emission spectra were taken on a PTI fluorometer (Photon Technology International, Trenton, NJ) at 20 °C. Chemical unfolding was performed by incubating proteins at 0.5 mg/mL in 25 mM Tris buffer (pH 8.5), 1 mM EDTA, 1 mM DTT, and 0−6 M guanidine hydrochloride (GuHCl) at 37 °C for 2 h and 4 °C overnight. Treated proteins in a 1-mm path length cuvette were then monitored using an excitation wavelength of 295 nm and emission spectra over a range of wavelengths from 310 to 420 nm. Spectra were corrected for background fluorescence from buffer or the buffer having the same concentration of GuHCl.

RESULTS

Protein Stability. The thermal stability of γM7 and γM2b was measured by monitoring the loss of CD signals corresponding to the 218 nm minimum for the β-sheet under increasing temperature. As shown in Figure 1, the melting temperatures for γM7 and γM2b are 58 and 60 °C, respectively, significantly lower than those of mouse γS and human γD crystallins. Consistently, other γM-crystallins from Antarctic toothfish and bigeye tuna also showed substantially lower temperature stability than the γ-crystallins from *B. Taurus*.[40]

Structure Determination. The solution structure of γM7-crystallin from zebrafish has been determined using multidimensional NMR with a total of 1427 restraints, including 961

dx.doi.org/10.1021/bi400151c | *Biochemistry* 2013, 52, 3579−3587

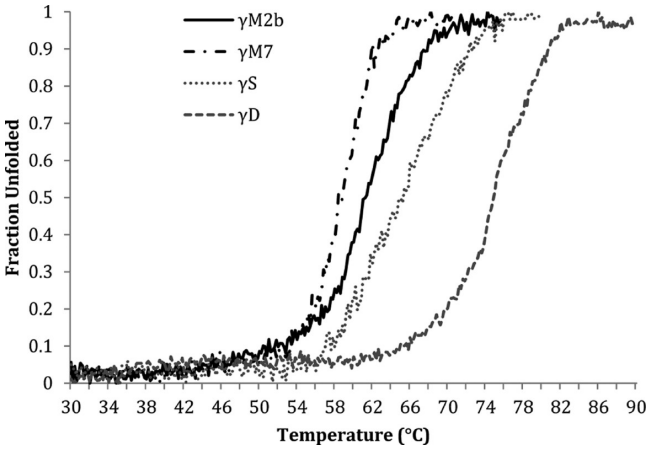

Figure 1. Temperature unfolding curves for γM7, γM2b, γS, and γD. Loss of secondary structure for zebrafish γM7, γM2b, mouse γS, and human γD-crystallins monitored by loss of CD signals at 218 nm, indicating lower heat stability for γM-crystallins.

interproton distances, 279 backbone dihedral angles, and 131 residual dipolar coupling constraints. Resonance assignments have been completed for 164 out of the 169 nonproline residues. Notably, the amide signals are missing from residues 10 to 13, spanning the region of the first β-hairpin loop between the β-strands 1 and 2. These vanishingly weak amide signals suggest that this region of γM7-crystallin experiences significant conformational exchange motion on the intermediate NMR time-scale that broadens the signals beyond the detection limit. An ensemble of the 15 lowest energy structures, superpositioned as shown in Figure 2, exhibits excellent

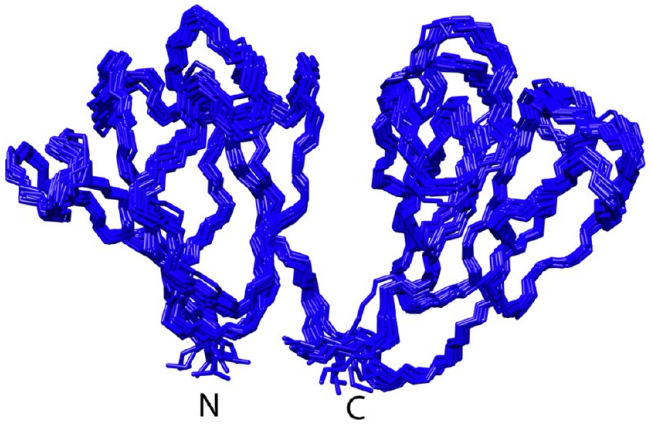

Figure 2. Superposition of 15 lowest energy NMR structures.

structural convergence with atomic root-mean-square deviations (rmsd's) of 0.48 ± 0.15 and 1.03 ± 0.10 Å with respect to the mean coordinate positions for the backbone and all heavy atoms, respectively. The structural statistics are summarized in Table 1.

Structure Comparison. γM7-Crystallin shows a two-domain architecture similar to that of previously determined γ-crystallin structures, with each domain possessing two intercalating Greek-key (GK) motifs. Figure 3A displays a comparison between the human γD-crystallin X-ray (PDB entry 1HK0) and the present solution structure, with the associated backbone rms differences being 1.51, 0.88, and 1.67 Å for the N- and C-terminal domains and the full length protein. With

Table 1. NMR Structural Statistics of γM7

NMR distance and dihedral constraints	
total constraints (per monomer)	1427
long range NOE ($5 \leq i - j$)	578
short range NOE ($1 < i - j < 5$)	129
sequential NOE	252
residual dipolar coupling	131
dihedral angle restraints: ϕ^a and ψ^a	279
hydrogen bond	56
structure statistics (20 structures)	
violation statistics	
distance constraints (Å)	0.040 ± 0.001
maximum distance violation (Å)	0.4
deviations from idealized covalent geometry	
bond lengths (Å)	0.0029 ± 0.0006
bond angles (deg)	0.473 ± 0.006
PROCHECK (Ramachandran plot)	
most favored region (%)	70.9
additionally allowed region (%)	26.5
generously allowed region (%)	2.0
disallowed region (%)	0.7
rms deviations from the average structure (Å)[b]	
backbone atoms	0.48
all heavy atoms	1.03

[a]The dihedral angle constraints ϕ and ψ were derived by using TALOS.[36] [b]rms deviations from the average structure were calculated for the residues Lys3−Ile171 of the final 15 structures.

respect to the NMR structure of murine γS-crystallin (PDB entry 1ZWM), similar backbone rmsd values, 1.53, 1.02, and 2.18 Å respectively, were also observed. Collectively, this indicates that the main structural difference between γM7 and mammalian lens crystallins is located in the N-terminal domain, while the C-terminal domains exhibit high structural similarity. As detailed in Figure 3B, the most noticeable structural difference between the fish γM7 and γD- or γS-crystallin resides within the variable loop 2 (VL2) in the N-terminal domain. This loop in γM7 is folded further away from the hydrophobic core compared to that of γD-crystallin. Evidently, the H^{α} of Met67 strongly NOE interacts with the H^{N} amide proton of Met72 (Figure 3C), replacing an otherwise i to i + 4 NOE pattern observed in the VL4 of γM7 and both VL2 and VL4 of mouse γS.[25] As a result, the aromatic side chain of Tyr66 tucks into the core of the N-terminal domain, making extensive hydrophobic contacts with the side chains of Ile36 and Val76. This conformation is in sharp contrast to the equivalent residues, His65 in γD- or Tyr69 in γS-crystallin, which project away from the domain and lack NOE interactions with the hydrophobic core residues.

The burying of Tyr66 is made possible by the absence of a tryptophan residue conservatively residing in VL2 in all lens γ-crystallins from mammals. This conserved tryptophan makes extensive contacts with the N-terminal hydrophobic core, so its absence in γM7 allows reoptimization of the hydrophobic interactions between residues in this loop and the N-terminal core. Consistent with this, instead of being highly solvent exposed like the equivalent Leu71 in γD-crystallin or Leu75 in γS, residue Met72 in γM7 protrudes into the hydrophobic core of the N-terminal domain, making extensive hydrophobic interactions. Leu75 of γS, on the contrary, shows very close methyl proton chemical shifts and virtually no inter-residue NOE cross-peak with any core residues. It is conceivable that

dx.doi.org/10.1021/bi400151c | Biochemistry 2013, 52, 3579−3587

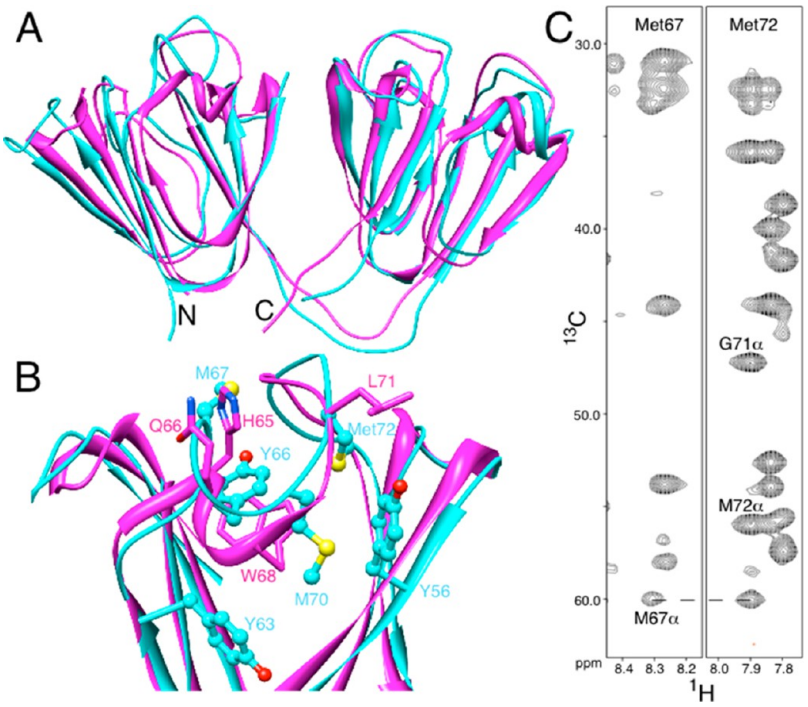

Figure 3. Overlay of γM7 NMR structure (cyan) with the X-ray γD-crystallin (1HK0, magenta) (A). A close view of the variable loop 2 in the N-terminal domain, which lacks a conserved tryptophan residue in γM7 (B), showing the comparison of the residues Tyr66, Met67, and Met72 from γM7, and their counterpart residues His65, Gln66, and Leu71 from γD, and the side chain interactions between Met70 with aromatic residues Tyr56 and Tyr63 in γM7. Stripes of 3D ^{15}N-edited NOESY showing the unusual *i* to *i* + 5 interaction observed in the VL2 of γM7 (C).

the increased hydrophobic packing by Tyr66 and Met72 in γM7 may at least in part compensate for the absence of the Trp residue, resulting in the altered loop conformation. Since all four GK motifs are structurally similar, we compared VL2 with the equivalent loops VL1 and VL3 that also lack a Trp residue. In a common sequence $\Phi(xxx)_{3-5}\Phi$, where the Φ represents a hydrophobic residue, the two equivalent flanking hydrophobic residues Leu26 and Phe30 in VL1 and Leu113 and Met119 in VL3 are all buried in a manner similar to that of Tyr66 and Met72 in VL2, further suggesting that a Trp residue is critical for dictating the VL conformation. A second conserved Trp located at the junction of two GK motifs in mammalian γ-crystallins is also missing in the N-terminal domain of γM7. It has been shown that this tryptophan plays an important structural role in stabilizing a corner conformation by forming a hydrogen bond between its side chain $H^{\varepsilon 1}$ (*i*) to the carbonyl oxygen at the *i*-3 position.[41] It is plausible that missing such an interaction may contribute to the decreased protein stability of zebrafish γM7 and other γM-crystallins, as shown in this study and for several examples from other fish.[40]

γM7 Exhibits Increased Backbone Dynamics in the Loop Regions. Next, we used NMR relaxation experiments to investigate the backbone motions of γM7. Figure 4 shows the comparison of the derived order parameters between γM7 and γS crystallins. Unlike γS, which exhibits quite uniform order parameters (S^2) for almost all residues (except those in the N- and C-terminal tails and the interdomain linker), γM7 shows much more variability. As shown in Figure 4, while all β-strands display similar S^2 values, lower values are observed for those primarily located in or near the loop regions, for example, VL1, VL2, VL4, and the first β-hairpin in the C-terminal domain. Together with the missing NH signal in the first β-hairpin, the relaxation measurement suggests that γM7 possesses higher

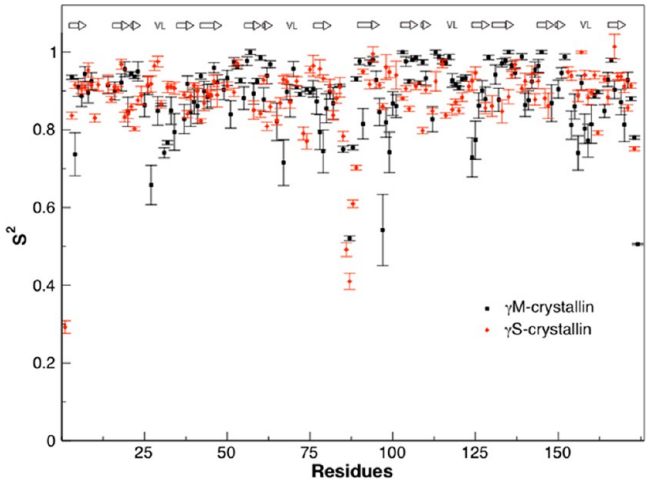

Figure 4. Comparison of backbone order parameter (s^2) of γM7 (black) and mouse γS (red) derived from ^{15}N relaxation experiments, indicating larger motions observed in the variable loop regions and comparatively lower dynamics in the interdomain linker in γM7 than γS. The arrows indicate β-stranded secondary structure and the variable loops between the 3rd and 4th β-strands in each Greek Key motif are noted as VL.

magnitude backbone conformational motion in the loop regions. When compared to the relaxation results of γD,[42] the loop regions of γM7 again appear to be more flexible. Furthermore, the amplitudes of internal motions of the interdomain linker among these three proteins vary significantly, with γS being the most flexible, followed by γM7 and then γD, which has order parameters similar to those of the residues in the N-/C-terminal structure core.[42] On the basis of the sequence alignment of these γ-crystallins (Figure 5A), it

dx.doi.org/10.1021/bi400151c | *Biochemistry* 2013, 52, 3579−3587

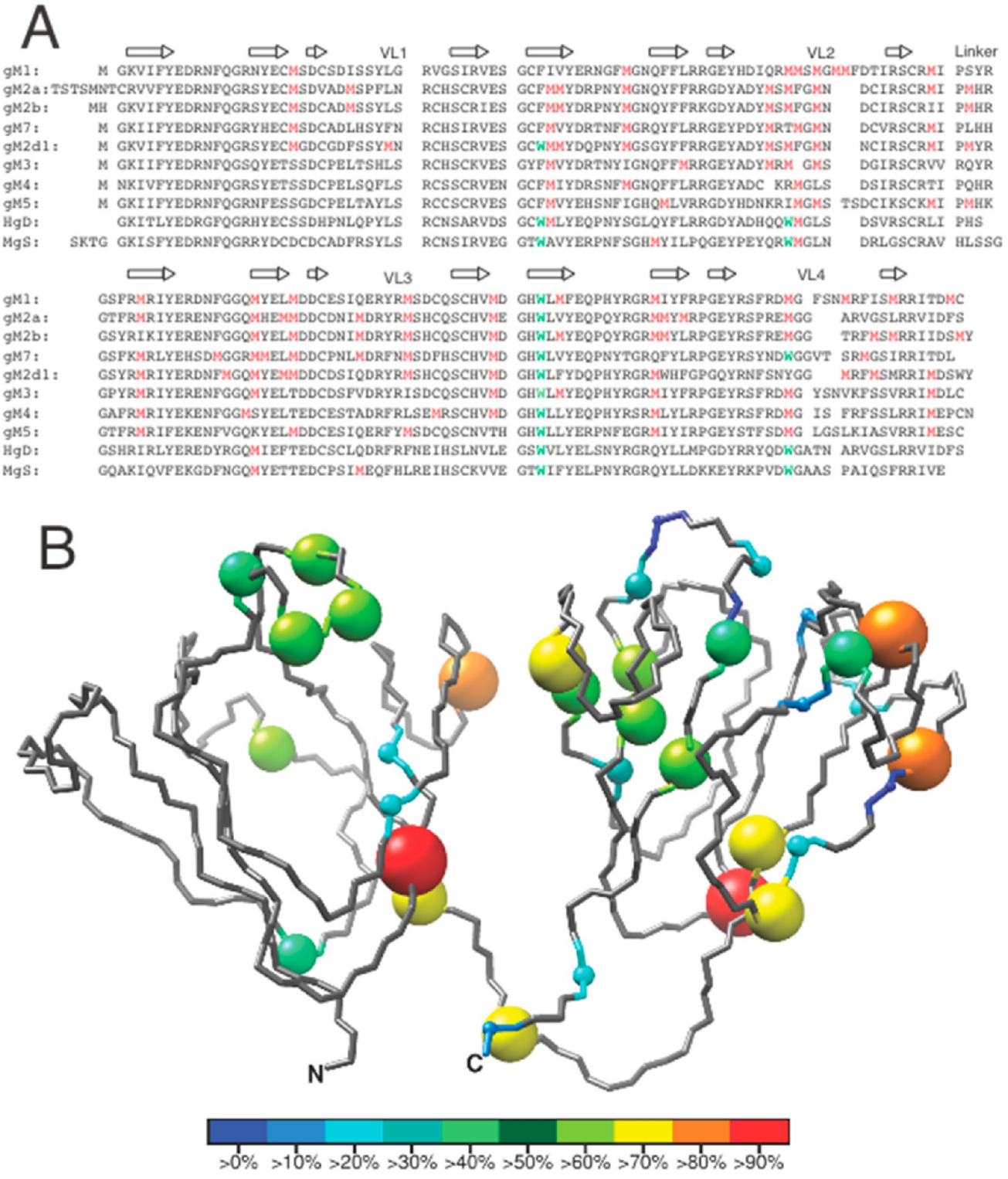

Figure 5. (A) Sequence alignment of fish γM- with human γD- and mouse γS-crystallins, with all of the methionine residues colored in red and tryptophan colored in green. (B) Methionine residues in 15 fish γM-crystallins are positioned on the NMR structure of γM7, with the size and color of the sphere corresponding to the frequency of the methionine occurrences.

appears that the flexibility of the interdomain linker correlates with its length, with a three residue-linker for γD, four for γM7, and five for γS. In γD, the short three-residue linker is as rigid as both of the structural domains.[42]

Methionine Residues in γM-Crystallins. An interesting feature of the fish γM-crystallins is their high methionine content, up to ∼15% of the total amino acid composition. Figure 5A shows the alignment of several γM-crystallins with the methionine residues highlighted, and Figure 5B positions all the methionine residues found in 15 fish γM-crystallins on the structure of γM7. Noticeably, more than 70% of the methionines are located in the second and the third GK motifs, whereas less than 10% are found in the first GK. Most of the methionine substitutions are located in the loops, turns, and

dx.doi.org/10.1021/bi400151c | *Biochemistry* 2013, 52, 3579−3587

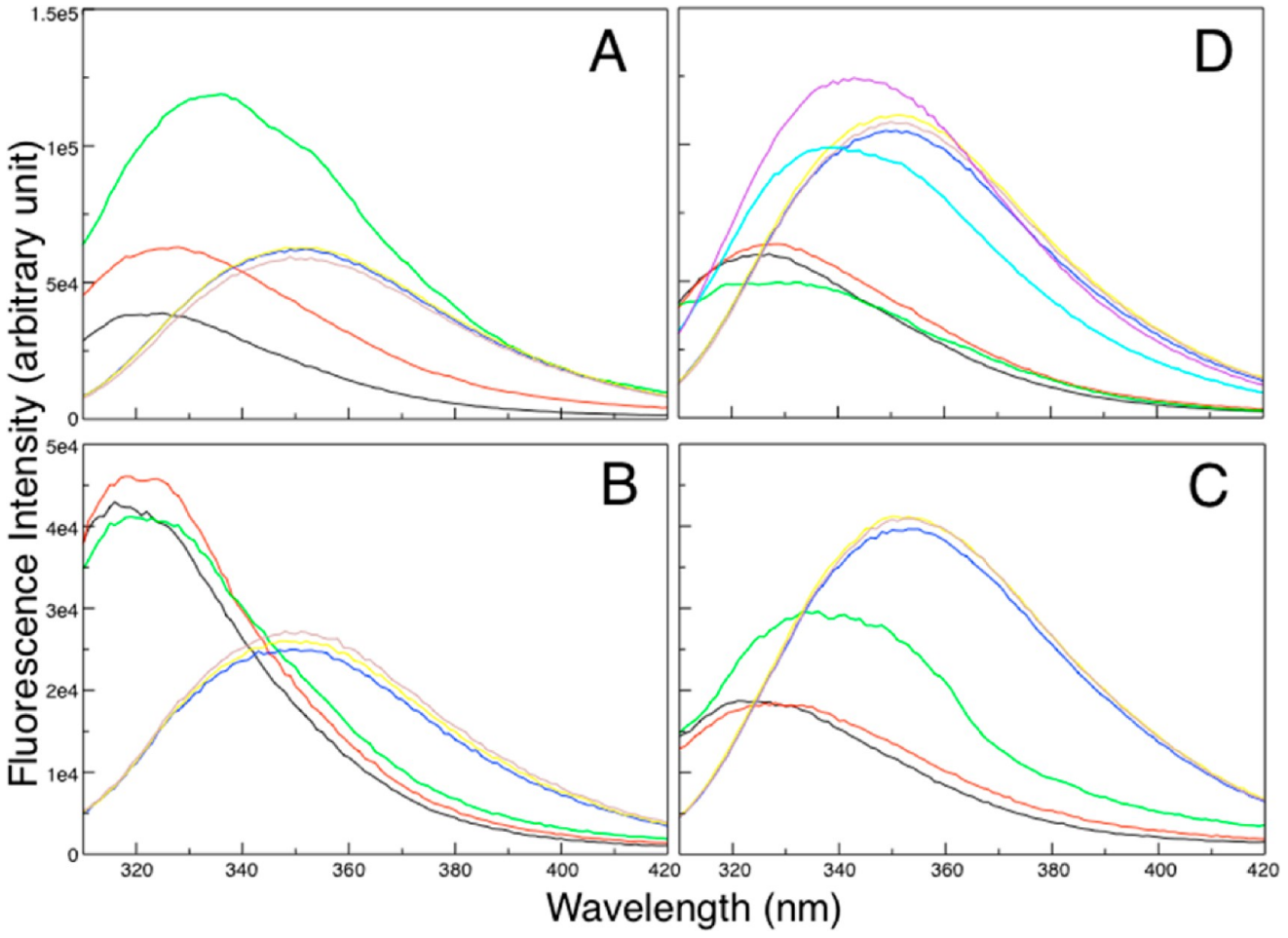

Figure 6. Representative typtophan fluorescence spectra of fish γM7 (A), γM2b (B), γM7 W132F (C), and γS (D) at 0 M (black), 0.4 M (red), 0.8 M (green), 3.0 M (blue), 4.0 M (yellow), and 5.0 M (brown) GuHCl. Since γS is more stable than γM7, the fluorescence profiles at 1.6 M (cyan) and 2.0 M (purple) are shown for γS in (D), showing that the fluorescence jump happened at higher GuHCl concentration than that in γM7.

on the edge of a β-sheet, particularly in the variable loops and on the second β-strand of the second, third, and fourth GK motifs. In γM7, except for Met44, Met91, and Met165, which are located in the domain interface and the center of the C-terminal hydrophobic core, all other methionines are at least partially, if not completely, solvent accessible. Interestingly, most of the exposed methionine side chains are not fully disordered. Out of 14 exposed methionine residues, 11 of them make strong to medium NOE contacts to at least one surface aromatic residue, making those methionine side chains attach to the surface of the protein instead of freely projecting into solution. For example, as shown in Figure 3B, the side chain of Met67 sits ∼5 Å above the aromatic ring of Tyr66 and ∼5 Å from that of His34, while that of Met70 makes simultaneous NOE contacts with Tyr56 and Tyr63, and both Met99 and Met103 interact with the aromatic ring of Tyr94 in the first β-hairpin of the C-terminal domain. This partial ordering of the exposed methionine side chains is consistent with the recent study suggesting that the methionine−aromatic interaction plays a key role in stabilizing protein structure.[43]

Protein Unfolding Monitored by Tryptophan Fluorescence. Unfolding of γM7-crystallin was monitored by intrinsic tryptophan fluorescence with increasing amounts of chemical denaturant, guanidinium hydrochloride (GuHCl). Given that the two tryptophan residues in γM7 are located in the C-terminal domain, their fluorescence change induced by GuHCl allowed us to monitor how a single βγ-domain unfolds in the content of a native two-domain protein. Interestingly, as shown in Figure 6A, the Trp fluorescence of γM7 initially increased with increasing GuHCl, accompanied by a slight red shift of the λ_{max}. The fluorescence reached its maximum intensity at about ∼0.8 M GuHCl, followed by a decrease with the increase of the GuHCl concentration until the protein was completely denatured. To further delineate the individual contribution to the overall fluorescence change of these two tryptophans, the unfolding of a homologous γM2b and W132F γM7 was monitored in the same manner. γM2b only contains the tryptophan at the conjunction of the third and fourth GK motifs. The Trp fluorescence profile of γM2b (Figure 6B) showed a continuous decrease upon denaturation, whereas that of W132F (Figure 6C) exhibited an increasing trend with the increase of denaturant concentration. A significant fluorescence jump at 0.8 M GuHCl appears to coincide with the initial fluorescence burst observed in WT γM7. These observations indicate that the local environments of the two tryptophans in a natively folded crystallin domain are different. The VL structure helps to effectively quench the fluorescence of Trp165, whereas Trp132 is more fluorescent when it is buried in the hydrophobic core. These distinct fluorescence profiles of each tryptophan were also observed in human γD- and γS-crystallins with one behaving as a fluorescence quencher and the other as a fluorescence enhancer.[8,9] On the basis of these observations,

dx.doi.org/10.1021/bi400151c | Biochemistry 2013, 52, 3579−3587

the initial increase in fluorescence of γM7 is likely due to local unfolding of the VL spanning between the β7 and β8, disrupting the key structure feature responsible for effective fluorescence quenching of Trp165. The fact that losing the quenching effect of Trp165 precedes any significant fluorescence change from the more buried Trp132 suggests that under low denaturant concentration a native-like structural core is maintained while the variable loops can be more readily unfolded.

To test whether the early unfolding of the variable loop observed for γM-crystallins is a common feature of lens γ-crystallins, we further investigated the denaturation of mouse γS-crystallin. As shown in Figure 6D, an early loss of fluorescence quenching effect was also observed for γS, followed by a decrease expected for further exposing the structurally buried Trp36 and Trp132, at higher GuHCl concentration. The fact that γS has a higher unfolding denaturant concentration again suggests that γM-crystallins are generally less stable than their counterparts in mammalian lenses. In summary, γ-crystallin domains may share a common unfolding pathway starting from the unfolding of the variable loops on the top of the wedged fold. This could partially expose the hydrophobic core of the γ-crystallin domain, potentially leading to protein aggregation.

DISCUSSION

The solution structure of zebrafish γM7-crystallin reveals the common two-domain, four-GK topology found in other γ (and β-)-crystallins.[44] These two domains, linked by a short linker, are stabilized by interdomain interactions between conserved hydrophobic residues located in the domain interface. This evolutionally conserved domain-pairing structure contributes to the high thermodynamic stability required for lens proteins.[2] However, compared to other known lens βγ-crystallin structures from mammals, significant structural differences were observed in the N-terminal domain of γM7 (Figure 3), particularly in the variable loop between the β7 and β8 strands (VL2). This difference seems to be due to the absence of a tryptophan residue, which is conserved in this region in other βγ-crystallins. As a consequence, the hydrophobic residues flanking VL2 reorganized to maximize hydrophobic packing, adopting a conformation similar to those structure-equivalent counterparts VL1 and VL3, which also lack a tryptophan. Apparently, the interaction between the tryptophan side chain and the domain core is critical for the specific conformation of the variable loop, which itself is key for effective fluorescence quenching of the tryptophan residue.[45] The C-terminal domain of γM7, however, maintains two conserved tryptophans and has a VL structure almost superimposable on that of γD and γS crystallins. On the basis of these results, it can be predicted that when the tryptophan in VL4 is missing, as in many other γM-crystallins (Figure 5A), the structure of the variable loop would also closely resemble that of VL2 of γM7.

In γ-crystallin and β-crystallin domains from mammals, the paired tryptophans are conserved in both N- and C-terminal domains. It has been proposed that these residues help absorb UV light between 295 and 400 nm, preventing it from reaching the retina, while escaping photodegradation themselves through a fast fluorescence quench mechanism.[8,9,45] Between the two tryptophans, the one located in the variable loop serves as the major mediator for the fast fluorescence quench,[8] whereas the other one, located at the bottom of the hydrophobic core, is likely to play a more important structural role by stabilizing the inter-GK connection.[25] Consistent with this proposition, irradiation of bovine γB-crystallin *in vitro* photodegrades Trp42 and Trp131 three times more efficiently than Trp68 and Trp157.[46] This UV role may be significant since cumulative exposure to UV radiation is correlated with the prevalence of senile cataract.[47] Compared to mammalian γ-crystallins, as shown in Figure 5A, only one tryptophan in the core of the C-terminal domain is highly conserved in all fish γM-crystallins, whereas the other three are completely dispensable. While the structural tryptophan in the N-terminal core is commonly replaced by a phenylalanine, interestingly, both tryptophans in the variable loop are frequently substituted by a methionine. The absence of these tryptophans in aquatic species, especially the high fluorescence quencher, may be related to the low exposure to UV light under water. Although γM-crystallins do not conserve the Trp pairs, they are present in fish γS-, γN- and β-crystallins.[48] The presence of the four Trp's in mammalian γA-F-crystallins, proteins of the lens core, may reflect the greater UV exposure of diurnal, land species.

The striking abundance of methionine residues in the γM-crystallins suggests some importance of this amino acid for the proteins. The observed lower heat stability of γM7-, γM2b-, and some other γM-crystallins indicates that high methionine content does not itself increase protein stability as speculated previously.[10] In general, the thermal stability of γ-crystallins appears to correlate with the body temperature,[40] with higher stability in mammalian crystallins. Alternatively, the flexibility of methionine side chains could facilitate intermolecular interactions.[11] Interestingly, as shown in Figure 5B, the VLs and β-strands with high methionine content in the second and fourth GKs contribute to the domain interface, while the equivalent regions on the third GK motif may potentially aid intermolecular interaction similar to intramolecular domain−domain interaction. Consistent with this notion, in the crystal structure of the tetrameric βB2-crystallin (2BB2), the same regions from the second, third, and fourth GK motifs are directly involved in interdomain interaction with other crystallin molecules.[49] Under the extreme protein density of the fish lens, the surface flexibility imparted by the methionine side chain may also contribute to their cold adaptation compared to those in mammals[7] possibly at the expense of their thermal stability.[40] The presence of a high content of methionine residues (and others) in γM-crystallins has also been suggested to contribute directly to the high refractive index requirement of the fish lens.[12] Consistent with this notion, as shown in Figure 5A, the positions frequently replaced by a methionine are commonly occupied by those with a lower refractive index increment, such as valine, alanine, isoleucine, and threonine, in mammalian lens γ-crystallins.[50] Together with the fact that other refractive proteins such as the S-crystallins from cephalopods[12] and the reflectins from squid[17] have also evolved to adopt extremely high methionine content, optimization of the refractive index seems to be at least one of the driving forces for methionine amino acid selection in lens-related proteins. Finally, our structure of γM7-crystallin indicates that the majority of the surface exposed methionines are in close proximity with at least one aromatic residue. Indeed, such interaction seems to be a common stabilizing factor in many proteins, while mutations disrupting the interaction are associated with several diseases.[43] In summary, it is conceivable that high methionine content in fish γM-crystallins is the result of an accumulative effect from the requirement of high refractive properties, coupled with a low

dx.doi.org/10.1021/bi400151c | *Biochemistry* 2013, 52, 3579−3587

temperature environment and high protein density. During evolution, the risk of oxidation of methionine residue, the reduced need for high refractive index, and the requirement for higher protein stability in mammals may have driven the substitution of methionine by other amino acids.

In order to investigate the consequences of Trp and Met content in fish γM-crystallins for higher backbone dynamics, NMR relaxation studies of γM7 were performed. These showed a noticeable difference in dynamics in surface loops among γM7, γS-,[25] and γD-crystallins[42] and revealed an interesting correlation between the fast local internal dynamics in the interdomain linker and its length. From a three-residue linker in γD to four-residues in γM7 and five-residues in γS, the motion of the linker increases. Interestingly, mouse γC has an isoform in mice in which the linker has an extra amino acid insertion, and it has been proposed that local motions in crystallins could provide entropic compensation for the restrictions of short-range order in lenses at high protein concentration.[25]

Tryptophan fluorescence of γM- and γS-crystallins showed a very interesting denaturation profile, exhibiting a distinct initial increase at low GuHCl concentration followed by a decrease to a level corresponding to a fully unfolded state. On the basis of the denaturation profile of each individual tryptophan in γM2b, W136F-γM7, and the single Trp mutants of γD and γS,[8,9] the initial fluorescence increase likely reflects loss of quenching by partial unfolding of the variable loop, while the later decrease corresponds to unfolding of the core of the βγ-crystallin domain. This unfolding mode perfectly agrees with our previous NMR results of the stability-impaired mouse γS-crystallin mutant, Opj, which revealed a partially unfolded intermediate with a native-like overall structure but a much more unfolded variable loop.[23] Consistent with our results, a single βγ-crystallin domain from a nonlenticular protein has recently been proposed to unfold through the formation of a native-like intermediate,[51] which exhibits elevated flexibility and higher propensity of forming insoluble aggregates.[51] It is noteworthy that these partially unfolded intermediates are structurally different from those proposed for human γD-crystallin, which sequentially unfolds the four GK motifs under increasing amounts of denaturant.[52] It is conceivable that the intermediate observed in current studies may represent an early stage of unfolding of a βγ-crystallin domain, which may promote further opening of individual GK motifs and ultimately lead to protein aggregation.[53]

AUTHOR INFORMATION

Corresponding Author

*Tel: 614-247-5040. Fax: 614-292-6773. E-mail: wu.473@osu.edu.

Author Contributions

§B.M. and Y.C. contributed equally to this work.

Funding

Z.W. is funded by NIH grant R21EY018423 and partially by grant R01AG031903. Y.C. and G.W. are funded by the NEI intramural program.

Notes

The authors declare no competing financial interest.

ACKNOWLEDGMENTS

We thank Dr. Keith Wyatt for subcloning the γM-crystallin cDNAs.

REFERENCES

(1) Bloemendal, H., de Jong, W., Jaenicke, R., Lubsen6, N. H., Slingsby, C., and Tardieu, A. (2004) Ageing and vision: structure, stability and function of lens crystallins. *Prog. Biophys. Mol. Biol. 86*, 407−485.

(2) Jaenicke, R. (1999) Stability and folding of domain proteins. *Prog. Biophys. Mol. Biol. 71*, 155−241.

(3) Purkiss, A. G., Bateman, O. A., Wyatt, K., Wilmarth, P. A., David, L. L., Wistow, G. J., and Slingsby, C. (2007) Biophysical properties of γC-crystallin in human and mouse eye lens: the role of molecular dipoles. *J. Mol. Biol. 372*, 205−222.

(4) White, H. E., Driessen, H. P., Slingsby, C., Moss, D. S., and Lindley, P. F. (1989) Packing interactions in the eye-lens. Structural analysis, internal symmetry and lattice interactions of bovine gamma IVa-Crystallin. *J. Mol. Biol. 207*, 217−235.

(5) Slingsby, C. (1985) Structural variation in lens crystallins. *Trends Biochem. Sci. 10*, 281−284.

(6) Pan, F. M., Chang, W. C., Chao, Y. K., and Chiou, S. H. (1994) Characterization of gamma-crystallins from a hybrid teleostean fish: multiplicity of isoforms as revealed by cDNA sequence analysis. *Biochem. Biophys. Res. Commun. 202*, 527−534.

(7) Kiss, A. J., and Cheng, C. H. (2008) Molecular diversity and genomic organisation of the alpha, beta and gamma eye lens crystallins from the Antarctic toothfish *Dissostichus mawsoni*. *Comp. Biochem. Physiol., Part D: Genomics Proteomics 3*, 155−171.

(8) Chen, J., Flaugh, S. L., Callis, P. R., and King, J. (2006) Mechanism of the highly efficient quenching of tryptophan fluorescence in human gammaD-Crystallin. *Biochemistry 45*, 11552−11563.

(9) Chen, J., Toptygin, D., Brand, L., and King, J. (2008) Mechanism of the efficient tryptophan fluorescence quenching in human gammaD-Crystallin studied by time-resolved fluorescence. *Biochemistry 47*, 10705−10721.

(10) Chang, T., Jiang, Y. J., Chiou, S. H., and Chang, W. C. (1988) Carp gamma-crystallins with high methionine content: cloning and sequencing of the complementary DNA. *Biochim. Biophys. Acta 951*, 226−229.

(11) Srikanthan, D., Bateman, O. A., Purkiss, A. G., and Slingsby, C. (2004) Sulfur in human crystallins. *Exp. Eye Res. 79*, 823−831.

(12) Zhao, H., Brown, P. H., Magone, M. T., and Schuck, P. (2012) The molecular refractive function of lens gamma-Crystallins. *J. Mol. Biol. 411*, 680−699.

(13) Kappe, G., Purkiss, A. G., van Genesen, S. T., Slingsby, C., and Lubsen, N. H. (2010) Explosive expansion of betagamma-Crystallin genes in the ancestral vertebrate. *J. Mol. Evol. 71*, 219−230.

(14) Zhao, H., Magone, M. T., and Schuck, P. (2012) The role of macromolecular crowding in the evolution of lens crystallins with high molecular refractive index. *Phys. Biol. 8*, 046004.

(15) Tomarev, S. I., Zinovieva, R. D., and Piatigorsky, J. (1991) Crystallins of the octopus lens. Recruitment from detoxification enzymes. *J. Biol. Chem. 266*, 24226−24231.

(16) Siezen, R. J., and Shaw, D. C. (1982) Physicochemical characterization of lens proteins of the squid *Nototodarus gouldi* and comparison with vertebrate crystallins. *Biochim. Biophys. Acta 704*, 304−320.

(17) Crookes, W. J., Ding, L. L., Huang, Q. L., Kimbell, J. R., Horwitz, J., and McFall-Ngai, M. J. (2004) Reflectins: the unusual proteins of squid reflective tissues. *Science 303*, 235−238.

(18) Kramer, R. M., Crookes-Goodson, W. J., and Naik, R. R. (2007) The self-organizing properties of squid reflectin protein. *Nat. Mater. 6*, 533−538.

(19) Mitraki, A., and King, J. (1989) Protein folding intermediates and inclusion body formation. *BioTechnology 7*, 690−697.

(20) Chiti, F., and Dobson, C. M. (2006) Protein misfolding, functional amyloid, and human disease. *Annu. Rev. Biochem. 75*, 333−366.

(21) Rudolph, R., Siebendritt, R., Nesslauer, G., Sharma, A. K., and Jaenicke, R. (1990) Folding of an all-β protein: independent domain

folding in γII-Crystallin from calf eye lens. *Proc. Natl. Acad. Sci. U.S.A. 87*, 4625−4629.
(22) Flaugh, S. L., Kosinski-collins, M. S., and King, J. (2005) Interdomain side-chain interactions in human γD Crystallin influencing folding and stability. *Protein Sci. 14*, 2030−2043.
(23) Mahler, B., Doddapaneni, K., Kleckner, I., Yuan, C., Wistow, G., and Wu, Z. (2011) Characterization of a transient unfolding intermediate in a core mutant of gammaS-Crystallin. *J. Mol. Biol. 405*, 840−850.
(24) Kosinski-collins, M. S., and King, J. (2003) In vitro unfolding, refolding, and polymerization of human γD Crystallin, a protein involved in cataract formation. *Protein Sci. 12*, 480−490.
(25) Wu, Z. R., Delaglio, F., Wyatt, M. K., Wistow, G., and Bax, A. (2005) Solution structure of γS-Crystallin by molecular fragment replacement NMR. *Protein Sci. 14*, 3101−3114.
(26) Sinha, D., Wyatt, M. K., Sarra, R., Jaworski, C., Slingsby, C., Thaung, C., Pannell, L., Robison, W. G., Favor, J., Lyon, M., and Wistow, G. (2001) A Temperature-sensitive mutation of Crygs in the murine Opj cataract. *J. Biol. Chem. 276*, 9308−9315.
(27) Pace, C. N., Shirley, B. A., and Thomson, J. A. (1989) Measuring the Conformational Stability of a Protein, in *Protein Structure: A Practical Approach* (Creighton, T. E., Ed.), pp 311−329, IRL Press, Oxford, U.K.
(28) Grzesiek, S., Dobeli, H., Gentz, R., Garotta, G., Labhardt, A. M., and Bax, A. (1992) ^{1}H, ^{13}C, and ^{15}N NMR backbone assignments and secondary structure of human interferon. *Biochemistry 31*, 8180−8190.
(29) Bax, A., and Grzesiek, S. (1993) Methodological advances in protein NMR. *Acc. Chem. Res. 26*, 131−138.
(30) Neri, D., Szyperski, T., Otting, G., Senn, H., and Wuthrich, K. (1989) Stereospecific nuclear magnetic resonance assignments of the methyl groups of valine and leucine in the DNA-binding domain of the 434 repressor by biosynthetically directed fractional ^{13}C labeling. *Biochemistry 28*, 7510−7516.
(31) Vuister, G. W., and Bax, A. (1992) Resolution enhancement and spectral editing of uniformly ^{13}C-enriched proteins by homonuclear broadband ^{13}C decoupling. *J. Magn. Reson. 98*, 428−435.
(32) Chou, J. J., Gaemers, S., Howder, B., Louis, J. M. L., and Bax, A. (2001) A simple apparatus for generating stretched polyacrylamide gels, yielding uniform alignment of proteins and detergent micelles. *J. Biomol. NMR 21*, 377−382.
(33) Farrow, N. A., Muhandiram, R., Singer, A. U., Pascal, S. M., Kay, C. M., Gish, G., Shoelson, S. E., Pawson, T., Forman-Kay, J. D., and Kay, L. E. (1994) Backbone dynamics of a free and a phosphopeptide-complexed Src homology 2 domain studied by ^{15}N NMR relaxation. *Biochemistry 33*, 5984−6003.
(34) Delaglio, F., Grzesiek, S., Vuister, G. W., Zhu, G., Pfeifer, J., and Bax, A. (1995) Nmrpipe - a multidimensional spectral processing system based on Unix Pipes. *J. Biomol. NMR 6*, 277−293.
(35) Johnson, B. A., and Blevins, R. A. (1994) NMRView: a computer program for the visualization and analysis of NMR data. *J. Biomol. NMR 4*, 603−614.
(36) Shirley, B. A., Stanssens, P., Steyaert, J., and Pace, C. N. (1989) Conformational stability and activity of ribonuclease T1 and mutants. Gln25——Lys, Glu58——Ala, and the double mutant. *J. Biol. Chem. 264*, 11621−11625.
(37) Schwieters, C., Kuszewski, J., Tjandra, N., and Clore, G. (2003) The Xplor-NIH NMR molecular structure determinsation package. *J. Magn. Resson. 160*, 65−73.
(38) Laskowski, R. A., Rullmann, J. A. C., MacArthur, M. W., Kaptein, R., and Thornton, J. M. (1996) AQUA and Procheck NMR: Programs for checking the quality of protein structures solved by NMR. *J. Biomol. NMR 8*, 477−486.
(39) Pettersen, E. F., Goddard, T. D., Huang, C. C., Couch, G. S., Greenblatt, D. M., Meng, E. C., and Ferrin, T. E. (2004) UCSF Chimera–a visualization system for exploratory research and analysis. *J. Comput. Chem. 25*, 1605−1612.
(40) Kiss, A. J., Mirarefi, A. Y., Ramakrishnan, S., Zukoski, C. F., Devries, A. L., and Cheng, C. H. (2004) Cold-stable eye lens crystallins of the Antarctic nototheniid toothfish *Dissostichus mawsoni* Norman. *J Exp Biol 207*, 4633−4649.
(41) Hemmingsen, J. M., Gernert, K. M., Richardson, J. S., and Richarson, D. C. (1994) The tyrosine corner: A feature of most Greek key (beta)-barrel proteins. *Protein Sci. 3*, 1927−1937.
(42) Jung, J., Byeon, I. J., Wang, Y., King, J., and Gronenborn, A. M. (2009) The structure of the cataract-causing P23T mutant of human γD-Crystallin exhibits distinctive local conformational and dynamic changes. *Biochemistry 48*, 2597−2609.
(43) Valley, C. C., Cembran, A., Perlmutter, J. D., Lewis, A. K., Labello, N. P., Gao, J., and Sachs, J. N. (2012) The methionine-aromatic motif plays a unique role in stabilizing protein structure. *J. Biol. Chem. 287*, 34979−34991.
(44) Blundell, T., Lindley, P. F., Miller, L., Moss, D., Slingsby, C., Tickle, I., Turnell, B., and Wistow, G. (1981) The molecular structure and stability of the eye lens: X-ray analysis of γ-Crystallin II. *Nature 289*, 771−777.
(45) Chen, J., Callis, P. R., and King, J. (2009) Mechanism of the very efficient quenching of tryptophan fluorescence in human gamma D- and gamma S-crystallins: the gamma-Crystallin fold may have evolved to protect tryptophan residues from ultraviolet photodamage. *Biochemistry 48*, 3708−3716.
(46) Tallmadge, D. H., and Borkman, R. F. (1990) The rates of photolysis of the four individual tryptophan residues in UV exposed calf gamma-II Crystallin. *Photochem. Photobiol. 51*, 363−368.
(47) Robman, L., and Taylor, H. (2005) External factors in the development of cataract. *Eye (London, U.K.) 19*, 1074−1082.
(48) Wistow, G., Wyatt, M. K., David, L., Gao, C., Bateman, O., Bernstein, S., Tomarev, S., Segovia, L., Slingsby, C., and Vihtelic, T. (2005) γN-Crystallin and the evolution of the βγ-Crystallin superfamily in vertebrates. *FEBS J. 272*, 2276−2291.
(49) Bax, B., Lapatto, R., Nalini, V., Driessen, H., Lindley, P. F., Mahadevan, D., Blundell, T. L., and Slingsby, C. (1990) X-ray analysis of beta B2-Crystallin and evolution of oligomeric lens proteins. *Nature 347*, 776−780.
(50) Zhao, H., Brown, P. H., and Schuck, P. (2012) On the distribution of protein refractive index increments. *Biophys. J. 100*, 2309−2317.
(51) Rajanikanth, V., Srivastava, S. S., Singh, A. K., Rajyalakshmi, M., Chandra, K., Aravind, P., Sankaranarayanan, R., and Sharma, Y. (2012) Aggregation-prone near-native intermediate formation during unfolding of a structurally similar nonlenticular betagamma-Crystallin domain. *Biochemistry 51*, 8502−8513.
(52) Mills, I. A., Flaugh, S. L., Kosinski-Collins, M. S., and King, J. A. (2007) Folding and stability of the isolated Greek key domains of the long-lived human lens proteins γD-Crystallin and γS-Crystallin. *Protein Sci. 16*, 2427−2444.
(53) Lee, S., Mahler, B., Toward, J., Jones, B., Wyatt, K., Dong, L., Wistow, G., and Wu, Z. (2010) A single destabilizing mutation (F9S) promotes concerted unfolding of an entire globular domain in γS-Crystallin. *J. Mol. Biol. 399*, 320−330.